ITC 2/54
Information Technology and Control
Vol. 54 / No. 2/ 2025
pp. 471-488
DOI 10.5755/j01.itc.54.2.37944

Method of Ship Target Oblique Frame Detection in Lightweight SAR Image Based on Recurrent Neural Network

Received 2024/07/08 | Accepted after revision 2024/11/23

HOW TO CITE: Huang, L., Zhu, X, Luo, B. (2025). Method of Ship Target Oblique Frame Detection in Lightweight SAR Image Based on Recurrent Neural Network. *Information Technology and Control*, 54(2), 471-488. https://doi.org/10.5755/j01.itc.54.2.37944

Method of Ship Target Oblique Frame Detection in Lightweight SAR Image Based on Recurrent Neural Network

Liang Huang*, Xufang Zhu, Bing Luo
College of Electronic Engineering, Naval University of Engineering, Wuhan 430033, China

Corresponding author: huangldsdas@163.com

When ship targets appear in SAR images at different angles, their shapes and contours may change significantly. At present, target box detection algorithms often match and recognize based on templates with fixed shapes and directions. When the angle of ship targets changes, these templates may no longer be applicable, leading to the decline of detection algorithm performance, and it is difficult to accurately identify and locate targets. Therefore, for the purpose of solving the problem of angle sensitivity, the method of ship target oblique frame detection in lightweight SAR image based on recurrent neural network is studied to improve the effect of ship target oblique frame detection. Using recurrent neural network, the framework of ship target oblique frame detection in lightweight SAR images is established to ensure the detection accuracy, significantly reduce the demand for computing resources, and achieve more efficient detection. In this framework, SAR images are input in the input layer and transmitted to the hidden layer. The lightweight convolutional neural network is used as the hidden layer, and channel attention mechanism is introduced to improve the extraction effect of useful ship target features. The output layer processes the ship target characteristics, predicts the ship target center point heat map, and calculates the oblique frame vertex coordinates of the center point heat map, so as to have better adaptability to the ship targets that tilt or rotate in the SAR image, solve the angle sensitivity problem, and complete the ship target oblique frame detection. The volume Kalman filter algorithm is used to train the recurrent neural network, optimize the network weight, and improve the detection accuracy of ship target oblique frame. Experiments show that this method can effectively extract ship target features. Under different background, this method can accurately detect the slant frame of ship target. Under different occlusion rates, the robustness of the method is better.

KEYWORDS: Recurrent neural network, Lightweight, SAR image, Ship target, Diagonal frame detection, Convolutional neural network

1. Introduction

Synthetic Aperture Radar (SAR), being a dynamic microwave imaging system, holds a pivotal position in various applications such as maritime surveillance, resource prospecting, military surveillance, and numerous other domains [5]. SAR has all-day and all-weather working ability, can penetrate clouds, and is not limited by lighting conditions, providing a reliable data source for ship target detection. However, due to the characteristics of SAR images [1], such as complex background noise, diversity of target shapes and scales, and different orientations and attitudes of targets in the images, accurate detection of ship targets has become a challenging task [2]. Traditional ship target detection methods mainly rely on manually designed features and threshold segmentation technology. These methods may achieve certain results in specific scenes, but their detection performance and robustness are often unsatisfactory in the face of complex and changeable SAR images [11]. Through the research of ship target detection methods in SAR images, real-time monitoring and early warning of sea targets can be achieved, which provides important information support for military decision-making. At the same time, it is also of great significance to monitor and crack down on illegal activities such as smuggling and illegal immigration, which is conducive to safeguarding national security and maritime rights and interests. Therefore, developing an efficient and precise approach for ship target detection in SAR imagery is of paramount theoretical importance and practical value. For example, Sheikh et al. [17] realized end-to-end target detection through YOLOv3 (You Only Look Once version 3). For the purpose of detecting ship targets in SAR images, YOLOv3 is optimized according to the characteristics of SAR image, including adjusting the network structure to adapt to the resolution and noise characteristics of SAR image, and optimizing the training strategy to improve the detection accuracy. The experimental outcomes demonstrate that the proposed method exhibits rapid and precise capabilities in target detection [17]. The predefined anchor frame of YOLOv3 is usually based on the horizontal or vertical direction, which makes it perform poorly when dealing with oblique or rotating frames, limiting its performance in angle sensitivity. When the target presents oblique or rotating attitude, YOLOv3 may not be able to accurately predict the angle of the target frame, resulting in a large deviation between the detection frame and the real target. Chandrakar et al. [2] combined the advantages of radial basis function (RBF) neural network in function approximation and nonlinear mapping, and the characteristics of fuzzy dynamic learning neural network (FDLNN) in dynamic learning and adaptability. By introducing cell division propagation (CBF) algorithm, they realized adaptive optimization of network structure and performance improvement. In the target detection task, this method can effectively extract the characteristics of the target, and achieve fast and accurate target detection. The method exhibits robust performance across diverse scenarios, as evidenced by the experimental results [3]. When optimizing the network structure, CBF algorithm mainly focuses on improving the generalization ability and learning efficiency of the network, and seldom considers the impact of angle changes on detection performance. Therefore, in the process of adaptive optimization of network structure, it may not be able to effectively adapt to the change of target angle, resulting in deviation between the detection frame and the real target. Ranjith et al. enhanced the robustness of the deep learning model against noise changes and interference factors by introducing robust training strategies and network structure optimization, and completed target detection. Extensive testing reveals that the method consistently delivers reliable outcomes in a range of demanding scenarios [14]. The robust deep learning model mainly focuses on the overall information of the target when extracting the target features, but may not be sensitive to the changes of the local details caused by angle changes. This may lead to the model being unable to accurately capture the boundary information of the target when detecting the oblique box or rotating box target, thus affecting the accuracy and stability of the detection box. Cherri et al. [4] combined the advantages of optical correlation technology and digital image processing to achieve efficient and accurate target detection. The joint transform correlator makes use of the parallel processing ability and spatial filtering characteristics of the optical system to jointly transform the input image and the reference image, and forms correlation peaks on the correlation plane, so as to achieve rapid target detection [4]. The joint transform correlator mainly relies on the spatial domain features of the image for matching and detection. When the angle of the target changes, its spatial domain characteristics will change accordingly, which may lead to significant changes in the position and intensity of the correlation peak. Due to the high sensitivity of joint transform correlator to spatial domain features, the change of angle may lead to the decline of detection performance, or even lead to false detection or missing detection. Yin et al. proposed an object detection and interpretation model based on gradient weighted class activation mapping and reinforcement learning to address the complex background of RSI, the lack of interpretability in existing object detection models, and the issues of feature extraction and object classification accuracy between different network structures and layers [23]. Firstly, using ResNet as the backbone network, extract the features of RSI and generate feature maps. Then, a global average pooling layer is added to obtain the feature weight vectors corresponding to the feature maps. The weighted vector is superimposed onto the output class activation mapping. Optimize the generated region generation network using reinforcement learning methods. At the same time, we improved the reward function of reinforcement learning and enhanced the effectiveness of the region generation network. However, this method failed to consider the significant changes in shape and contour that may occur in SAR image ship target oblique frame detection, resulting in a decrease in detection performance and difficulty in accurately detecting targets.

Nowadays, with the rapid development of deep learning technology, significant achievements have been made in its application in image processing and computer vision fields [22, 19]. Especially in object detection tasks, deep learning models have become the mainstream method. For example, Zheng et al. [24] developed a deep convolutional autoencoder (MR-DCAE) model based on manifold regularization, which optimized a specially designed autoencoder (AE) through entropy stochastic gradient descent, and then used the reconstruction error in the testing phase to determine the parameter settings of the model to improve its performance. Zheng et al. [25] introduced a pruning method called Drop path to reduce the model parameters of 2D deep CNNs. Given a trained deep CNN, different lengths of pruning paths can be achieved by ranking the impact of each layer of neurons on the model's possible approximate correct (PAC) Bayesian boundary. The results show that Drop path achieves significant model compression and acceleration, with negligible accuracy loss. These models are capable of automatically learning complex feature representations from data, achieving unprecedented performance in various visual tasks. However, although deep learning has made some progress in object detection, there are still some challenges, namely, targets in SAR images often have different angles and scales, which require models to have strong rotation and scale invariance. Deep learning models have not considered the issue of angle sensitivity in detection, resulting in poor detection accuracy in ship target oblique frame detection in AR images. Recurrent neural network is a neural network model that can process sequential or hierarchical data [21]. It can maintain the continuity of information in the whole sequence. This feature enables recurrent neural network to make full use of context information in SAR images and improve the accuracy of target detection. Context information is very important for ship target detection, which can help the model better understand the shape, scale and orientation of the target. Because ships may present different orientations and attitudes in SAR images, the target frame may appear as a slanted frame rather than a traditional vertical frame. Recurrent neural network can capture this sequential change [20], solve the problem of angle sensitivity, and improve detection performance. Based on this, in order to solve the problem of poor detection accuracy when ship targets appear in SAR images from different angles, this study proposes a lightweight SAR image ship target oblique frame detection method based on recurrent neural networks, which promotes the development of the SAR image ship target detection field. This method uses a lightweight convolutional neural network as the hidden layer and introduces a channel attention mechanism. This mechanism utilizes global information to enhance the extraction of useful ship target information features and suppress useless features, thereby filtering out high-quality information and making the entire hidden layer more efficient in extracting ship target features. Based on this, the ship target features are processed through the output layer to predict the center point heatmap of the ship target, and the coordinates of the oblique box vertices of the center point heatmap are calculated to have better adaptability to ship targets that appear tilted or rotated in SAR images, solve the problem of angle sensitivity, and complete ship target oblique box detection. The volume Kalman filter algorithm is a Gaussian filtering method based on Bayesian filtering theory, which has high accuracy and stability when dealing with nonlinear systems. Therefore, in order to further improve the accuracy of ship target oblique frame detection, the volumetric Kalman filter algorithm is adopted to train a recurrent neural network and optimize the network weights. In this process, the volumetric Kalman filter algorithm approximates the Gaussian integral of nonlinear functions by using volumetric rules, which enables it to provide higher estimation accuracy than traditional Kalman filters when dealing with nonlinear systems. It can more accurately estimate the network state and parameters, thereby improving the accuracy of ship target oblique frame detection. At the same time, the volumetric Kalman filter algorithm can effectively resist the influence of errors and measurement noise. During the RNN training process, it helps to maintain the stability and generalization ability of the network, and can maintain good detection performance even in the presence of noise or uncertainty. And the volume Kalman filter algorithm approximates the state distribution through volume points, which is more efficient in computation than other nonlinear filtering methods. In RNN, it can reduce the computational burden during the training process and accelerate the convergence speed of the network. Thus, accurate and efficient SAR image ship target oblique frame detection can be achieved.

2. Implementation of Ship Target Oblique Frame Detection in Lightweight SAR Images Based on Recursive Neural Network

SAR images usually contain a large amount of data and information, which will face the problems of high computational complexity and slow processing speed in detection. Recurrent neural network has the ability to process time series data, and combined with lightweight design, it can improve the processing speed and efficiency while ensuring the detection accuracy. At the same time, ships may show various angles in SAR images, especially oblique attitude. The detection framework based on recurrent neural network can better adapt to this angle change and accurately detect oblique frame targets. In addition, recurrent neural network has advantages in feature extraction and learning ability, which can automatically learn the deep level features. Therefore, the recurrent neural network is used to establish a lightweight SAR image ship target oblique frame detection framework to ensure the detection accuracy, significantly reduce the demand for computing resources, and achieve more efficient detection. Finally, in order to further improve the accuracy of ship target oblique frame detection, the volume Kalman filter algorithm is used to train the recurrent neural network, optimize the network weight, and complete accurate and efficient ship target oblique frame detection in SAR images.

2.1. Lightweight SAR Image Ship Target Oblique Frame Detection Framework

The recurrent neural network is used to detect the ship target slant frame in the lightweight SAR image. The detection framework is shown in Figure 1.

Figure 1

Skew frame detection frame of ship target in lightweight SAR image.

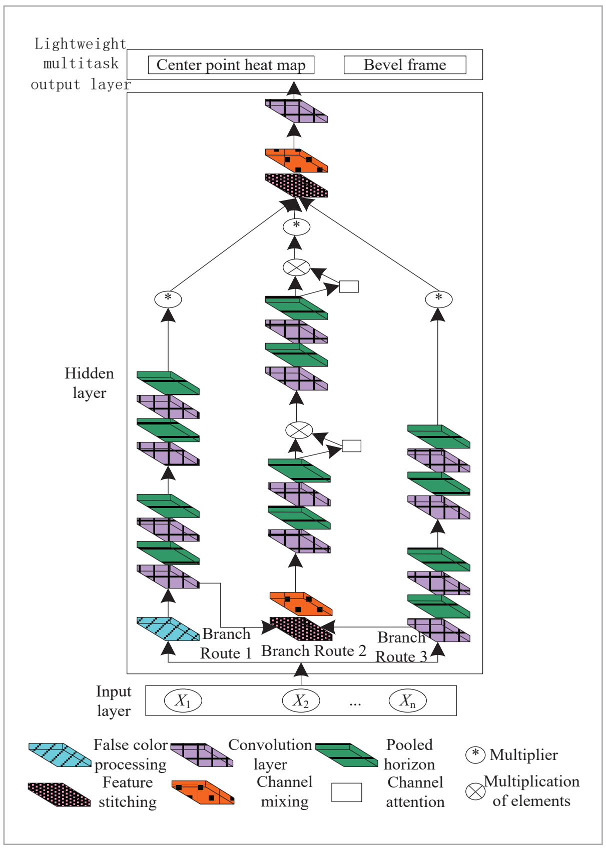

This framework uses a lightweight convolutional neural network as the hidden layer and introduces channel attention mechanism to improve the feature extraction performance of ship targets, providing reliable support for subsequent detection. Then, in order to have better adaptability to ship targets that appear tilted or rotated in SAR images, the center point heatmap of the ship target is predicted, and the coordinates of the oblique box vertices of the center point heatmap are calculated to solve the angle sensitivity problem and zcomplete ship target oblique box detection. In the detection framework, the specific implementation process is described as follows: first input SAR images in the input layer $X=\{X_1, X_2 \cdots, X_n\}$, where the number of SAR images is n. Then, the lightweight convolutional neural network is used as the hidden layer to extract ship target features in the SAR image. Finally, through the lightweight multitask output layer, the target center point heat map and oblique frame parameters are predicted to complete the ship target oblique frame detection in the lightweight SAR image.

2.2 Hidden Layer of Ship Target Oblique Frame Detection in Lightweight SAR Image

In the lightweight SAR image oblique frame detection framework in Section 2.1, in order to improve the feature extraction effect of ship targets in SAR images, the lightweight convolutional neural network is used as the hidden layer to replace the traditional hidden layer [15].

In recurrent neural network, the output of the input layer is:

$$\beta_i^t = W_{nm} X_i^t + b_h . \tag{1}$$

Among them, X_i^t is for t moment, the i th SAR images; W_{nm} represents the matrix of weights that connects the input layer to the hidden layer; the n is the number of nodes in the input layer; the m is the number of nodes in the implicit layer; the b_n is the implicit layer bias.

Perform deep convolution operations to SAR image output of input layer β_i^t, applying a single convolution kernel to each channel, the input size of sample β_i^t is set to $\hat{W} \times A \times H$, of which, $\hat{W}$ is SAR image height; A is the width of SAR image; H is the number of SAR image channels. The convolution kernel of 3×3×1 is selected here, after H convolution operation, we get number of $H\hat{W} \times A$ ship target feature map. Point-by-point convolution is similar to normal convolution [16], and the number of channels can be adjusted. The convolution kernel size is set to 1×1×3, the number is set to N, then you end up with size of $\hat{W} \times A \times H$ ship target characterization map.

The corresponding calculations is:

$$3 \times 3 \times H \times \hat{W} \times A + H \times N \times \hat{W} \times A . \tag{2}$$

The standard convolution corresponds to the computation is:

$$3 \times 3 \times H \times N \times \hat{W} \times A . \tag{3}$$

Comparing the computational effort of deeply separable convolution with that of ordinary convolution, the following ratio is obtained:

$$\frac{3 \times 3 \times H \times \hat{W} \times A + H \times N \times \hat{W} \times A}{3 \times 3 \times H \times N \times \hat{W} \times A} = \frac{1}{N} + \frac{1}{3^2}. \tag{4}$$

From the above formula, when the size of convolution kernel is 3×3, the depth separable convolution can reduce the parameter reduce the parameter count to approximately 1/9 of that of ordinary convolution, which greatly increases the operation speed of the network, so the depth separable convolution is used in the paper in the construction of hidden layer.

Starting from the ship target feature map, the hidden layer of the recurrent neural network [8] combines ship target feature maps from different branches with concat function, but the features obtained by splicing can only be added in the channel, and the information flow is not smooth. Although it is possible to use 1×1 convolution to mix the information between channels, it will lead to the problem of a substantial increase in the number of parameters. However, channel shuffling can complete the information mixing between channels without increasing the amount of calculation and parameters, enhance the classification effect, and improve the detection accuracy of ship target oblique frame in lightweight SAR images [10]. Therefore, this paper uses channel shuffling operation to integrate branch information and improve the efficiency of hidden layer operation.

The channel attention mechanism SE (Squeeze and Exception) module is a response mechanism to adaptively recalibrates channel features by understanding the correlation between channels. This mechanism uses global information to enhance the extraction of useful ship target information features and suppress useless features [7]. The compression and excitation steps occur prior to the summation of features within the same branch.

Make Z as the input ship target feature map of SE module, that is, the ship target feature map extracted by depth separable convolution [6], and the feature mapping conversion operation is as follows:

$$F: Z \rightarrow U; Z \in R^{\hat{W}\times A\times H}, U \in R^{\hat{W}'\times A'\times H'}. \tag{5}$$

Among them, U is the feature mapping for Z. F is a mapping function; the R is a vector space; the A' is the height of the ship's target feature map after mapping transformation; and H' is the number of channels after mapping conversion, the $\hat{W}'$ is the width of the ship target feature map after mapping transformation; Use Equation (6) to get the Squeeze input:

$$u_h = v_h * Z. \tag{6}$$

Among them, * denotes the convolution; the v_h is the h th convolutional kernels. u_h is the h th two-dimensional matrix in U. Using Equation (7) global average pooling ($F_1(\cdot)$ operation) the matrix $\hat{W}'\times A'\times H'$ is compressed to $1\times 1\times H'$, whose compression essence is to represent all channel information with a uniform descriptor, statistic the h th elements in ξ (i.e. SAR image global information) can be calculated by Formula (7):

$$\xi_h = \frac{\sum_{i'=1}^{\hat{W}'}\sum_{j'=1}^{K'} u_h(i', j')}{\hat{W}'\times A'}, \tag{7}$$

where, $u_h(i', j')$ is the ship target feature map whose converted height is j' and the width is i'.

Based on the inter-channel correlation dependence, the compressed information is modeled as an expansion of the channel relationship through Equation (8):

$$s = \phi\left(\omega\phi\left(\omega\xi_h\right)\right). \tag{8}$$

Among them, ω is the weights. ϕ is a ReLU (Rectified Linear Unit) function, which is a special gating function. When modeling, the full connection layer is used to maintain a high degree of nonlinearity and flexibility, to achieve a low parameter high fitting restoration of hidden layer transformation. Finally, multiply the weight value obtained by expansion processing by the original matrix to obtain the recalibrated network output, that is, use Formula (9) to calculate the channel weight s_h with ship target characterization maps u_h by channel multiply.

$$\hat{z}_h = s_h u_h. \tag{9}$$

The channel attention mechanism SE module is used to filter out high-quality information, so that the whole hidden layer can extract ship target features more efficiently, $\hat{z}_h$ is the ship target feature map obtained from high-quality SAR images.

To achieve the lightweight of convolutional neural network, it is necessary to maximize the network efficiency in a simpler way [12]. The ConcatNet proposed in this paper is mainly implemented by feature splicing ϖ_1, ϖ_2 and ϖ_3 wewighting factors for each of the 3 branches, respectively.

For the purpose of enriching the dimension of feature input, the SAR image output from the input layer is divided into two channels in this paper: one channel inputs the SAR image after pseudo color processing to obtain its color map features, three channels input directly, two channels are processed in parallel separately, after a convolution layer, the output ship target feature maps are spliced together to form two channels, and feature stitching is completed using Concat function. However, Concat function can only complete the superposition of channel numbers, and cannot complete the integration of the information of the two branches. Therefore, channel shuffling is used to process the ship target feature map after splicing.

The convolution layer of 1, 2 and 3 branches of the hidden layer of recurrent neural network for feature extraction of ship targets is composed of 4 3×3 convolution layers, the difference is the number of convolution cores. The number of branch 1 convolution cores is 32, 32, 64, and 128, the number of branch 2 convolution cores is 96, 192, 384, and 384, the number of branch 3convolution cores is 64, 64, 128, and 256, respectively. A maximum pooling is added after the first three convolution layers of the branch to remove redundant information [18]. Due to the fact that fully connected layers typically contain a large number of parameters, not only does it increase the complexity of the model, but it may also lead to overfitting. Global average pooling simplifies the model structure by directly operating on the feature map, reducing the number of parameters. And global average pooling performs an average operation on the entire feature map, which helps to have stronger robustness to spatial transformations (such as translation and rotation) of the input image, preserving the spatial structural information of the feature map. Therefore, a global average pooling is added after the fourth convolution layer to replace the full connection layer, the feature map of ship target is reduced to one dimension. For the purpose of reducing the parameters of the network and complete the lightweight of the convolutional neural network [9], the hidden layer adopts depth separable convolution. In order to enhance the ship target feature extraction ability of branches, the limited computing power is used on important ship target features. Considering that the convolution operation itself contains spatial attention [13], it is proposed to add two channel attention mechanism SE modules on each branch to suppress useless information in the channel domain.

The process of establishing the hidden layer involves distinct and precise steps outlined below: first, the output values of the three branches are concatenated with Concat function and the ship target features are combined. The three channels are superimposed, and the channel attention mechanism SE module is added. Before the characteristics of the concatenated ship target are input, screening is performed to amplify the features of the useful branches. Then, the utilization of channel mixing techniques is employed to augment the exchange of informational flow across various channels. Finally, 1×1 convolutional layer is used to replace the full connection layer for classification to avoid destroying the spatial structure of SAR images, and the size of the input SAR images will not be limited. So far, the hidden layer has been constructed.

2.3 Output Layer of Ship Target Oblique Frame Detection in Lightweight SAR Image

In the detection framework of Subsection 2.1, the lightweight multitasking output layer, including the centroid heat map prediction branch and the slant frame parameter prediction branch, only adds two layers of convolution on the 4-fold downsampled ship target feature map output from the implicit layer in Subsection 2.2, and the output channels of the second layer of convolution correspond to the number of predicted parameters. Among them, the number of output channels of the centroid heat map prediction branch is 1, and the number of output channels of the diagonal frame parameter prediction branch is 8.

The slant frame is represented by the center point and the slant frame parameters. Next, in order to have better adaptability to the ship target with tilt or rotation in the SAR image and solve the angle sensitivity problem, the center point heat map and the slant frame parameter prediction branch in the lightweight multitask output layer are respectively corresponding to predict the ship target center point heat map, and calculate the slant frame vertex coordinates of the center point heat map, complete effective ship target oblique frame detection.

The centroid heatmap of the lightweight multitasking output layer output is:

$$g_t = \psi\left(\hat{z}_h\right). \tag{10}$$

Among them, ψ is the activation function from the implicit layer to the output layer.

Center point heat map g_t make the coordinates of the center point of the ship target rounded by 4 times downsampling are taken as positive samples. Since the number of positive samples is small, to ensure a balanced representation of positive and negative samples, the center point of the ship target is taken as the origin, the central point heat map g_t remaining position (x, y) is treated using a Gaussian kernel:

$$Y_{xy} = e^{-\frac{\left(x-q_x\right)^2+\left(y-q_y\right)^2}{2\lambda^2}}. \tag{11}$$

Among them, Y_{xy} is the value at the coordinates (x, y). (q_x, q_y) is the rounding coordinate after four times down sampling of the center point in the ship target feature map extracted from the SAR image in Section 2.2; λ is the adaptive scale factor.

Given the distinct feature of high aspect ratios exhibited by ship targets in SAR imagery, the direct use of angle regression slant frame has angle sensitivity, which results in unstable training process and low detection accuracy. When there is a slight deviation in the angle, the intersection of Union (IoU) drops sharply. The larger the aspect ratio, the sharper the decline.

To solve the problem of angular sensitivity, the diagonal frame is represented in the form of a rotation vector. With the short side as the width and the long side as the height, around the y axis rotated counterclockwise as positive, the angle is noted as α, clockwise rotation is negative, and the angle range is [-90°,90°).

The oblique box is represented by the rotation vector (p, r, d, l) from 4 edges to the center point q. First, the coordinate q' of q in the vertical border is obtained according to the coordinate rotation matrix:

$$q' = \frac{q}{R}. \tag{12}$$

Among them, $R = \begin{bmatrix} \cos\alpha & \sin\alpha \\ -\sin\alpha & \cos\alpha \end{bmatrix}$ is the rotation matrix.

Based on q' to obtain the vertical vector $\left(\hat{p}, \hat{r}, \hat{d}, \hat{l}\right)$, of which $\hat{p}$ is the vertical vector from the top edge to q', $\hat{r}$ is the vertical vector from the right to q', $\hat{d}$ is the vertical vector from the bottom edge to q', $\hat{l}$ is the vertical vectors from the left to q'. After that the rotation matrix is utilized to get the rotation vector of (p, r, d, l) from the 4 edges to q:

$$\left(p, r, d, l\right) = R\left(\hat{p}, \hat{r}, \hat{d}, \hat{l}\right). \tag{13}$$

Among them, $R = \begin{bmatrix} \cos\alpha & -\sin\alpha \\ \sin\alpha & \cos\alpha \end{bmatrix}$ is the rotation matrix.

The calculation formula for the vertex coordinates of the slanted frame of the ship target in SAR image is:

$$\begin{cases} o_1 = p + l + q \\ o_2 = p + r + q \\ o_3 = d + r + q \\ o_4 = d + l + q \end{cases}. \tag{14}$$

The slant frame is directly represented by a rotation vector whose coordinates are rounded from four edges to the center point, and the center point offset is reflected in the rotation vector, without the center point offset prediction branch, which simplifies the process of ship target slant frame detection in lightweight SAR images and reduces the detection frame parameters. Employing oblique box labeling offers a more precise depiction of the ship target's shape and orientation, minimizing unnecessary interference and facilitating the acquisition of crucial attribute information, including heading and aspect ratio. In SAR images, because ships may appear in different angles and postures, slant frame detection can be more flexible to adapt to these changes, and enhance the precision and dependability in the detection process.

2.4 Recurrent Neural Network Training Method for Ship Target Oblique Frame Detection in Lightweight SAR Image

Cubature Kalman filter (CKF) is a Gaussian filtering method based on Bayesian filtering theory, particularly suitable for state estimation of nonlinear systems. The core idea of CKF is to use a set of cubic points to approximate the Gaussian integral of the state distribution. These volume points are generated through symmetric volume rules, which are uniformly distributed in the state space and can accurately approximate the mean and covariance of a Gaussian distribution. CKF has a wide range of applications in the field of target tracking, especially in dealing with nonlinear motion models and Gaussian noise. For example, in radar or sonar systems, CKF can be used to track the position and velocity of moving targets. In inertial navigation systems (INS), CKF can be used to fuse measurement data from accelerometers and gyroscopes to estimate the attitude, velocity, and position of the carrier. In summary, the volume Kalman filter is a powerful nonlinear state estimation tool that has a wide range of applications in multiple fields. In SAR image ship target oblique frame detection, based on the advantages of CKF processing nonlinear systems, effectively resisting the influence of errors and measurement noise, and reducing the computational burden during training, in order to further improve the accuracy of ship target oblique frame detection, CKF is used to train the recurrent neural network detection framework constructed in Section 2.1, optimizing the weights of the input layer and the weights in the hidden layer of Section 2.2, to achieve accurate and efficient SAR image ship target oblique frame detection.

Taking the weights of the input layer,and the weights of the 3 branches of the implicit layer in Subsection 2.2 ϖ_1, ϖ_2 and ϖ_3 as the state variable of the ω, the output of the recurrent neural network g_t as observations to model the state space of recurrent neural networks.

The number of node layers of the recurrent neural network is L layers, with each layer labeled, respectively, as 1, 2, ⋯ , L, then the number of layers of weights is $L-1$, make $\omega_{\hat{i},\hat{j}}^{\gamma}$ as the connection weights for γ layer nodes $\left(\hat{i},\hat{j}\right)$. In order to introduce Kalman filtering into the training of recurrent neural networks, the recurrent neural network structure is abstracted into state space vectors ω. The state space model of a recurrent neural network is represented as follows:

$$\omega_{t+1} = \omega_t + \sigma_t \tag{15}$$

$$g_t = \psi\left(\omega_t, \hat{z}_h\right) + \delta_t, \tag{16}$$

of which, the weights of the network at time t+1 are determined by the weights at time t together with the process noise, the σ_t is the transfer noise with zero mean. δ_t is the measurement noise with zero mean.

Let the initial state as well as the initial covariance of the recurrent neural network be, respectively, the $\tilde{\omega}_{t|t}$ and $Q_{t|t}$, the implementation process of using CKF to train recurrent neural network is as follows:

1 Generate the volume transformation points of the state vector of the recurrent neural network according to the principle of volume transformation.

$$\omega_{t|t,\tau} = chol\left(Q_{t|t}\right)\chi_\tau + \tilde{\omega}_{t|t}. \tag{17}$$

Among them, χ_τ is a volumetric transformation point; the τ is the dimensionality of the state space of the recurrent neural network; the $chol(\cdot)$ is decompose for Cholesky.

2 The individual volume points obtained from the transformation are transferred according to Equation (15), to obtain the state estimation for t+1 moment.

$$\tilde{\omega}_{t+1|t} = \sum_\tau \frac{\omega_{t|t,\tau}}{2\eta}. \tag{18}$$

Among them, η is the total number of dimensions of the state space of the recurrent neural network.

3 Calculate the state estimation covariance matrices for t+1 moment:

$$Q_{t+1|t} = Q_{t|t} + \rho_{\sigma_t}^2. \tag{19}$$

Among them, ρ_{σ_t} is the covariance array for σ_t.

4 Generate measured volume transformation points for t+1 moment:

$$\omega'_{t+1|t,\tau} = chol\left(Q_{t+1|t}\right)\chi_\tau + \tilde{\omega}_{t+1|t}. \tag{20}$$

5 Each of the measured volumetric transformation points will be measured and predicted according to Equation (16):

$$\hat{G}_{t+1|t,\tau} = \psi\left(\omega'_{t+1t,\tau}, \hat{z}_h\right). \tag{21}$$

6 Solve measurement predictions and corresponding covariances for t+1 moment:

$$\hat{G}_{t+1|t} = \sum_\tau \frac{\hat{G}_{t+1|t,\tau}}{2\eta} \tag{22}$$

$$Q'_{t+1|t} = \sum_\tau \frac{\hat{G}_{t+1|t,\tau}\left(\hat{G}_{t+1|t,\tau}\right)^T}{2\eta} - \hat{G}_{t+1|t}\left(\hat{G}_{t+1|t}\right)^T + \rho_{\delta_t}^2 \tag{23}$$

$$Q''_{t+1|t} = \sum_\tau \frac{\omega'_{t+1|t,\tau}\left(\hat{G}_{t+1|t,\tau}\right)^T}{2\eta} - \tilde{\omega}_{t+1|t}\left(\hat{G}_{t+1|t}\right)^T \tag{24}$$

Among them, ρ_{δ_t} is the covariance array for δ_t; the T is a transpose symbol; the $Q'_{t+1|t}$ is the covariance of the residuals; the $Q''_{t+1|t}$ is the reciprocal covariance.

7 Calculate filter gain for t+1 moment:

$$\mu_{t+1} = \frac{Q''_{t+1|t}}{Q'_{t+1|t}}. \tag{25}$$

8 Complete updates of state vectors of recurrent neural networks for t+1 moment:

$$\tilde{\omega}_{t+1|t+1} = \tilde{\omega}_{t+1|t} + \mu_{t+1}\left(g_t - \hat{G}_{t+1|t}\right). \tag{26}$$

$\tilde{\omega}_{t+1|t+1}$ in Equation (26), is the state vector of the recurrent neural network after optimization, i.e., the optimized recurrent neural network weights.

To sum up, finalize the training of the recurrent neural network detection framework by fine-tuning the weights in both the input and hidden layers, replace the optimized weights back to the recurrent neural network, and complete accurate and efficient ship target oblique frame detection in SAR images.

3. Experimental Analysis

3.1. Experimental Setup

To verify the effectiveness of the proposed method, experimental testing is now conducted. The experimental platform scene is shown in Figure 2.

The experimental object is the SAR image dataset in the SARShip dataset, which is a multi-source SAR ship detection dataset. It uses domestically produced Gaofen-3 SAR images and Sentinel-1 images, covers multiple resolutions and polarization modes, and contains a large number of ship samples. It is very suitable for ship detection tasks in SAR images. The relevant parameters of the SAR image dataset are shown in Table 1.

Figure 2
Schematic diagram of experimental platform scene.

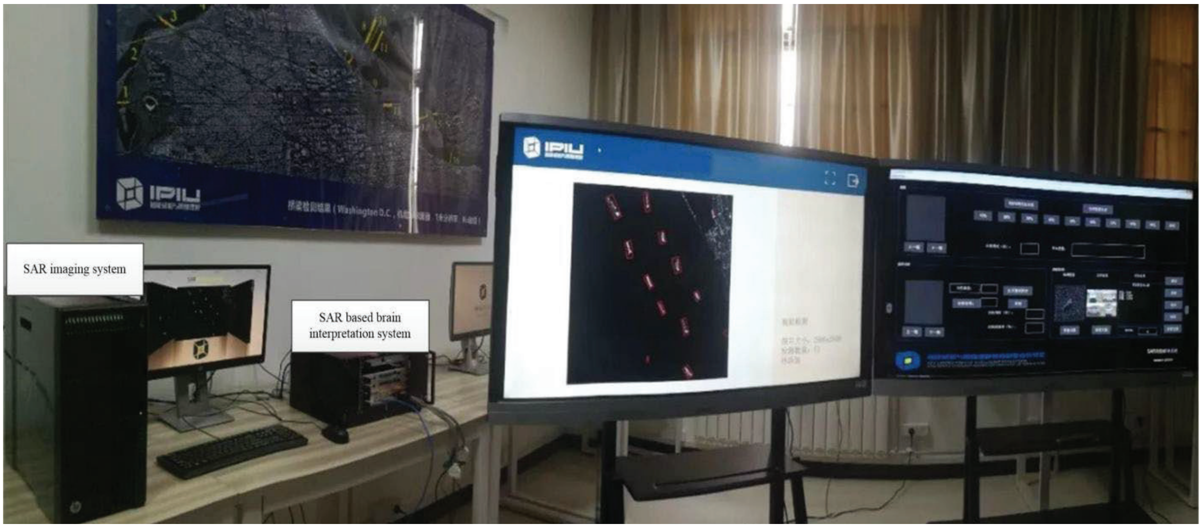

Table 1
Data set parameters.

Parameter name	Numerical range
Pulse repetition rate	100-10000 Hz
Pulse width	1-100 μs
Azimuth sampling rate	100-10000 Hz
Range resolution	1-10 m
Azimuth resolution	1-10 m
Imaging mode	UFS, FSI, QPSI, QPSII, FSII
Polarization mode	HH, VV, HV, VH
Frequency band	X-band, C-band, L-band
Image size	30× 30-120 ×120 pixels

Randomly select 1000 SAR image data from this dataset, and divide the SAR image data into training and testing sets in a 1:2 ratio. Randomly select two SAR images with complex and simple backgrounds in the test dataset, as shown in Figure 3.

Figure 3
SAR images.

(a) Complex background (b) Simple background

3.2. Indicator Setting

Since the feature extraction effect has a moderate impact on the subsequent detection, to assess the effectiveness of our proposed method, analyzing its feature extraction performance as a critical evaluation metric.

Matthews Correlation Coefficient (MCC) is an evaluation metric used to measure the performance of binary classification models. It considers the effects of true positives, true negatives, false positives, and false negatives, and can effectively evaluate the robustness of methods in the face of occlusion interference. In ship target detection, there may be a large number of background areas and a small number of ship target areas, resulting in class imbalance. MCC is insensitive to class imbalance and can fairly evaluate the performance of the model on different categories, making it particularly suitable for class imbalance situations and providing a comprehensive performance evaluation. Therefore, MCC is selected as the evaluation index to verify the strong robustness of the proposed method to interference such as occlusion, and to measure the accuracy of ship target oblique frame detection of the method. Its value is close to 1, indicating that the accuracy of ship target oblique frame detection is high. The MCC calculation formula is as follows.

$$MCC = \frac{TP \times TN - FP \times FN}{\sqrt{(TP+FP)\times(TP+FN)\times(TN+FP)\times(TN+FN)}}. \quad (27)$$

In the formula, TP stands for true positives, referring to the count of samples accurately identified as positive cases. TN stands for true negatives, indicating the number of samples correctly classified as negative cases. FP represents false positives, the count of samples incorrectly labeled as positive despite being negative. FN represents false negatives, where positive samples are wrongly predicted as negative.

To further demonstrate the merits of our proposed method, we validate its target detection performance visually, examining the presence of missed detections and false positives in ship target detection within SAR images.

To verify the real-time processing capability of the proposed method in practical applications, the detection efficiency is measured by the detection time. Using the tic toc function in MATLAB software to record the running time of the detection method is equal to the detection time of the method. The shorter it is, the higher the efficiency of the method in performing detection tasks.

3.3 Analysis of Results

3.3.1 Validity Analysis

Utilizing the technique presented in this paper, the SAR image depicted in Figure 3 is processed in pseudocolor, and the resulting output is displayed in Figure 4.

Figure 4

Pseudo-color processing results of SAR images with complex background and simple background.

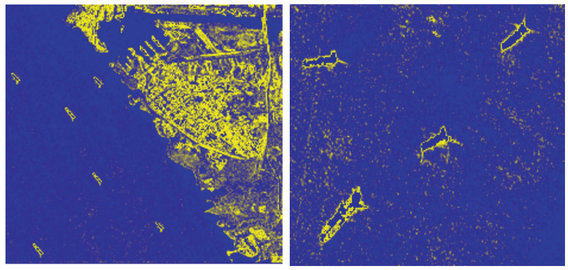

(a) Complex background (b) Simple background

It can be seen from the analysis of Figure 4 that this method can effectively perform pseudo color processing on SAR images with complex background and simple background to obtain color SAR images.

Using Figure 3(b) as an illustrative case, the methodology presented in this paper is employed to extract ship target features from this SAR image, and the extracted ship target features are subject to t-SNE dimension reduction visualization processing. The effect of ship target feature extraction in this method is analyzed, and the visualization processing results are shown in Figure 5.

Analyzing the situation of extracting ship target features from SAR images in the traditional hidden layer in Figure 5(a), we can see that there are some obvious limitations. First, the boundary between shape features and size features is blurred, which is mainly because the traditional hidden layer may not fully capture the subtle differences of ship targets when processing complex SAR images. In SAR images, the shape and size of a ship is an important feature for identifying its type, and the confusion of the bound-

Figure 5
Visual results of ship target features.

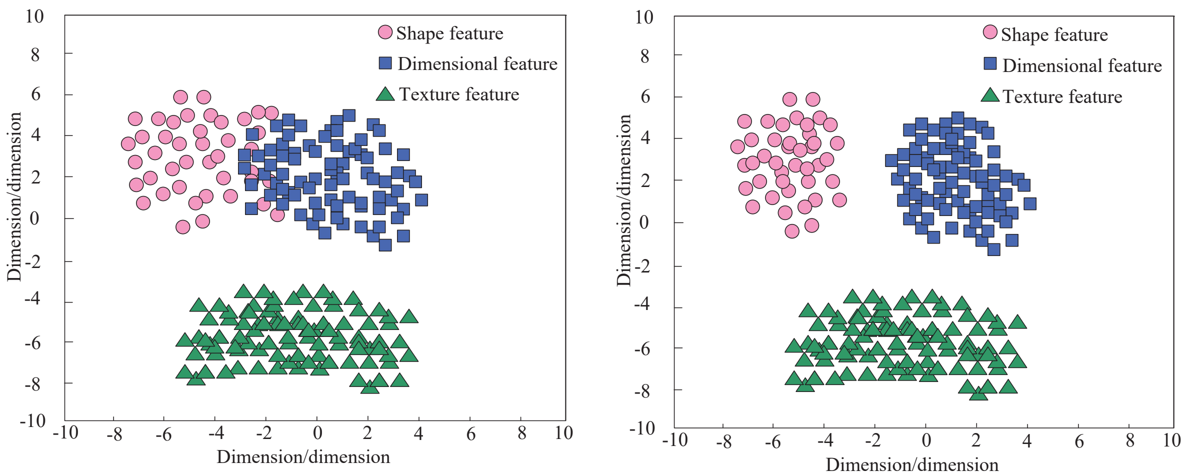

(a) Visual results of ship target features of traditional hidden layer

(b) Improve the visualization results of ship target features in the hidden layer

ary will make it difficult to accurately detect the ship target in the output layer. Diagonal frame detection usually depends on the accurate extraction and classification of target features. If inaccuracies occur during feature extraction, the precision of oblique frame detection will be significantly compromised. Consequently, the traditional hidden layer may fall short of fulfilling the demands for high-accuracy oblique frame detection when it comes to processing ship target feature extraction in SAR images. Analyzing Figure 5(b), we can clearly see the advantages of this method after improving the hidden layer by using lightweight convolutional neural network. The boundary between the three types of ship target features becomes very clear without any confusion. This is due to the powerful feature extraction ability of lightweight convolutional neural network, which can more deeply mine the information in SAR images and capture the subtle differences of ship targets. This improvement not only improves the accuracy of ship target feature extraction, but also provides more powerful support for subsequent oblique frame detection. Because the boundary between features is clear, the output layer can detect ship targets more accurately, thus improving the accuracy of oblique frame detection. In addition, the introduction of lightweight convolutional neural network may also bring advantages in computing efficiency, making the whole process more efficient.

3.3.2. Anti-jamming Robustness Analysis

For the purpose of verifying the robustness of this method to occlusion and other interferences, an artificial occlusion is created on a single image in the SAR image data set to test, and Matthews coefficient is used to measure the detection accuracy of ship target oblique frame in this method. For the real detection frame of each target in the image, according to the occlusion rate of the target $p \in (0,1]$ to design artificial shading. For target real detection frame with sizes of $\hat{W}\times A$, in which a piece of randomly selected dimensions of $p\hat{W}\times pA$ region, all the pixel values in the region are taken to be 0, which constitutes artificial occlusion, and the target occlusion rate is taken to be 0.1, 0.2, 0.3, 0.4, 0.5, respectively, to analyze the robustness of the ship target slanting frame detection under the occlusion interference with the introduction of different network layers within the method in this paper, and the outcomes of the testing are presented in Table 2.

Analyzing Table 2, it can be seen that when using different network layers for ship target oblique frame detection, the difficulty of ship target detection gradually increases with the increase of the

Table 2
Robustness test results of the proposed method for different target occlusion ratios.

Network layer	Shading ratio				
	0.1	0.2	0.3	0.4	0.5
Conventional hidden layer	0.85	0.81	0.74	0.69	0.62
Lightweight convolutional neural network (Common Convolutional)	0.88	0.84	0.77	0.72	0.65
Deep separable Convolutions	0.92	0.88	0.81	0.76	0.69
Deep separable convolutions + channel attention mechanisms	0.94	0.91	0.83	0.78	0.75
Deep separable convolutions + channel attention mechanism + Angle regression	0.97	0.94	0.86	0.83	0.79
Lightweight convolutional neural networks (depth separable convolutions) + channel attention mechanism + slant frame representation	0.99	0.96	0.94	0.93	0.92

occlusion rate, resulting in a decreasing trend of the Mathews coefficient. This is because the occlusion will lead to the loss of feature information of the ship target, which increases the difficulty of the detection method to distinguish the target from the background. However, when the traditional hidden layer is replaced by a lightweight convolutional neural network, the Mathews coefficient increases under different occlusion rates. This is attributed to the efficient feature extraction capability of lightweight convolutional neural networks, which can reduce the computation amount while retaining or even improving the feature expressiveness. This improvement allows the detection algorithm to maintain high detection accuracy in complex situations such as occlusion. Further, when depth-separable convolution is employed as a substitute for standard convolution, the Matthews correlation coefficient exhibits a consistent enhancement. By separating the spatial convolution and channel convolution, the depth-separable convolution not only reduces the computational complexity, but also improves the generalization ability of the model. This improvement enables the detection algorithm to extract key features more accurately when dealing with ship targets with different occlusion rates, thus improving the detection accuracy. In addition, the introduction of the channel attention mechanism leads to a further augmentation in the Mathews coefficient. The channel attention mechanism can adaptively adjust the weights between different channels, which makes the recurrent neural network pay more attention to the feature channels that are favorable to the detection task. This helps to detect ship targets more accurately in complex backgrounds, especially in the case of high occlusion rate, and can effectively suppress the influence of background noise and interferences. Finally, after the angular regression is replaced by the oblique frame representation, the Matthews coefficient of the oblique frame detection of ship targets is further improved. This is because the oblique frame representation can more accurately describe the tilt angle and position information of the ship target, which solves the angular sensitivity problem in angular regression. This improvement makes the detection method more accurate in detecting the ship target, which improves the detection accuracy. The above analysis shows that the improvement of the network layer in this paper effectively improves the Mathews coefficient of the ship target slant frame detection, and has better robustness of the ship target slant frame detection.

3.3.3 Analysis of the Effectiveness of Target Diagonal Frame Detection

Taking the target detection method in literature [17] YOLOv3, the target detection method using RBF-FDLNN and CBF algorithm in literature [3], the target detection method using robust depth learning in literature [14], and the target detection method using joint transform correlator in literature [4] as the comparison methods of the methods in this paper, the ship target oblique frame detection is carried out on the SAR image in Figure 3 using the above five methods, and the detection results of the target oblique frame are shown in Figures 6-7. As shown in Figures 8-10, the red box in the figure is the correct detected ship target, and the green box is the missed target.

Figure 6
Ship target detection results of the proposed method.

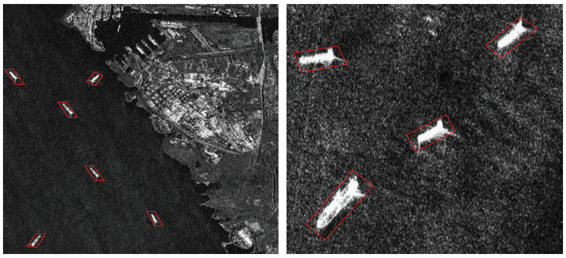

(a) Complex background (b) Simple background

Figure 7
Ship target detection results of the method in reference [17].

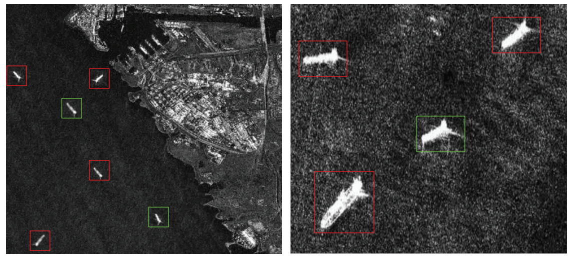

(a) Complex background (b) Simple background

Figure 8
Ship target detection results of the method in reference [3].

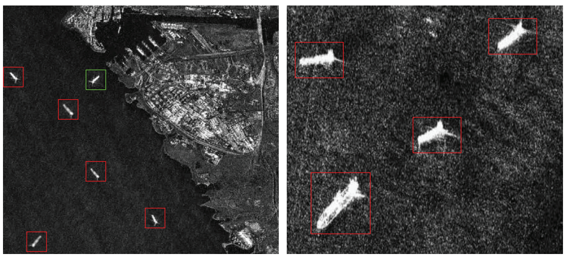

(a) Complex background (b) Simple background

Figure 9
Ship target detection results of the method in reference [14].

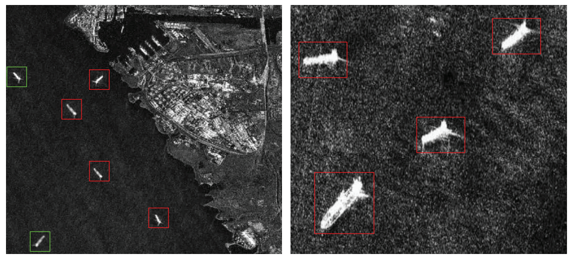

(a) Complex background (b) Simple background

Figure 10
Ship target detection results of the method in reference [4].

(a) Complex background (b) Simple background

Considering the analysis presented in Figures 6(a)-(b), for SAR images with complex background and simple background, this method can effectively complete ship target oblique frame detection, and the detection results are completely correct. Considering the analysis presented in Figures 7(a)-(b), in the complex background SAR image, there are two missing cases in the literature [17] method, and one missing case in the simple background SAR image. From the analysis of Figures 8(a)-(b), we can see that in the SAR image with complex background, the method in literature [3] has a missed detection, and the detection result of the target in the SAR image with simple background is completely correct. From the analysis of Figures 9 (a)-(b), we can see that in the complex background SAR image, there are two missed detection cases in the literature [14] method, and the detection result of the target in the simple background SAR image is completely correct. Considering the analysis presented in Figures 10(a)-(b), in the complex background SAR image, there are three missed cases in the literature [4] method, and one missed case in the simple background SAR image. The comprehensive analysis shows that the ship target detection accuracy of this method is the highest.

Based on the above tests, in order to further verify the detection performance of the proposed method, target occlusion rates of 0.1, 0.2, 0.3, 0.4, and 0.5 were taken in complex and simple backgrounds, respectively. The YOLOv3 object detection method in reference [17], the RBF-FDLNN and CBF algorithm object detection method in reference [3], the robust deep learning object detection method in reference [14], the joint transform correlator object detection method in reference [4], and the proposed method were used for ship object detection. Measure the detection effectiveness of each method using detection accuracy. Therefore, the accuracy of ship target detection under different occlusion rates using various methods is shown in Table 3.

Table 3

Results of ship target detection accuracy under different occlusion rates.

Background	Target occlusion rate/%	Accuracy of YOLOv3 object detection method/%	Accuracy of Object Detection Methods for RBF-FDLNN and CBF Algorithms/%	Accuracy of robust deep learning object detection methods/%	Accuracy of object detection method using joint transform correlators/%	Accuracy of the proposed method/%
Simple Background	0.1	93.3	96.5	94.2	92.4	99.7
	0.2	90.0	93.1	91.8	89.0	96.5
	0.3	86.9	90.5	87.3	86.6	94.2
	0.4	83.1	87.8	83.7	82.1	93.9
	0.5	77.9	85.2	78.1	77.6	92.6
Complex Background	0.1	92.1	95.3	92.8	90.5	98.4
	0.2	88.6	92.7	89.4	86.0	95.1
	0.3	84.0	88.1	85.7	81.4	93.8
	0.4	75.4	83.5	80.0	74.7	92.4
	0.5	70.7	77.7	75.1	67.1	91.0

According to the results in Table 3, it can be seen that there is a certain gap in the detection results when using the above five methods without background. The detection accuracy in simple backgrounds is always higher than that in complex backgrounds for ship target detection. And as the target occlusion rate increases, the accuracy of detection shows a decreasing trend regardless of the background used for detection. By comparing the results presented in Table 3, it can be concluded that the proposed method has higher detection accuracy than the other four comparison methods in different backgrounds as the target occlusion rate increases. In a simple background, when the target occlusion rate reaches a maximum of 0.5, the detection accuracy of the proposed method is 92.6%. However, the detection accuracy of YOLOv3's object detection method in reference [17], the object detection method using RBF-FDLNN and CBF algorithms in reference [3], the object detection method using robust deep learning in reference [14], and the object detection method using joint transform correlators in reference [4] are 77.9%, 85.2%, 78.1%, and 77.6%, respectively; In complex backgrounds, when the target occlusion rate reaches a maximum of 0.5, the detection accuracy of the proposed method is 91.0%. However, the detection accuracy of YOLOv3's object detection method in reference [17], the object detection method using RBF-FDLNN and CBF algorithms in reference [3], the object detection method using robust deep learning in reference [14], and the object detection method using joint transform correlators in reference [4] are 70.7%, 77.7%, 75.1%, and 67.1%, respectively. By comparison, it can be seen that the detection accuracy of the proposed method can consistently maintain above 90%, indicating good detection performance.

3.3.4 Efficiency Analysis of Target Oblique Frame Detection

To verify the detection efficiency of various methods in processing large amounts of SAR data and demonstrate the real-time processing capability of detection methods in practical applications, an analysis of detection efficiency is now conducted based on the results of detection time consumption. Then, the proposed method, YOLOv3's object detection method from reference [17], RBF-FDLNN and CBF algorithm's object detection method from reference [3], robust deep learning's object detection method from reference [14], and joint transform correlator's object detection method from reference [4] were used to detect a large number of SAR data samples. The detection time results of each method are shown in Table 4.

Table 4
Time consumption results of each method for detection.

Number of SAR data samples	Detection time/s				
	Proposed method	Object detection method for YOLOv3	Object detection methods using RBF-FDLNN and CBF algorithms	Robust deep learning based object detection method	Object detection method using joint transformation correlators
500	3.32	5.87	4.76	5.44	5.98
1000	5.28	9.28	7.35	8.97	10.76
1500	8.67	13.92	11.84	12.95	14.95
2000	10.95	17.98	15.18	16.73	18.87
2500	13.42	22.15	19.94	21.32	23.53
3000	16.17	26.84	23.25	25.47	27.96

According to the results in Table 4, it can be seen that when using the above five methods for large-scale SAR data sample detection tasks, the detection time shows an upward trend with the increase of sample size. However, compared with the object detection method of YOLOv3 in reference [17], the object detection method using RBF-FDLNN and CBF algorithms in reference [3], the object detection method using robust deep learning in reference [14], and the object detection method using joint transform correlators in reference [4] have lower detection time. When the number of SAR data samples reaches 3000, the detection time of the proposed method is less than 17 seconds, while the detection time of the four literature methods is all over 23 seconds. The comparison of the detection time results obtained from the five methods shows that the proposed method has high detection efficiency, low detection time when processing large amounts of SAR data, and strong real-time processing capability in practical applications.

4. Conclusion

After thorough research and experimentation, the lightweight SAR image-based approach for ship target slant frame detection utilizing recurrent neural networks has yielded outstanding outcomes. This methodology effectively captures sequential information through recurrent neural networks, leveraging the contextual details within SAR images to enhance the precision of ship target detection. Especially when dealing with complex situations such as occlusion, recurrent neural network can effectively detect the continuity and integrity of ship targets, providing an efficient and accurate solution for ship target detection in SAR images, indicating its broad application prospects and significant practical value in a wide range of fields. However, in extremely complex or heavily occluded scenes, the detection performance of the proposed method may decrease. Therefore, in order to further improve and optimize the detection performance of the proposed method, multimodal fusion technology will be explored in the future, combining SAR images and other sensor data (such as optical images) to provide richer information, improve detection accuracy, and make it more suitable for ship target oblique frame detection tasks in practical applications.

References

1. Bandi, S., Anbarasan, M., Sheela, D. Fusion of SAR and Optical Images Using Pixel-Based CNN. Neural Network World, 2022, 32(4), 197-213. https://doi.org/10.14311/NNW.2022.27.012
2. Chandrakar, R., Raja, R., Miri, R., Patra, R. K., Sinha, U. Computer Succoured Vaticination of Multi-Object Detection and Histogram Enhancement in Low Vision. International Journal of Biometrics, 2023, 15(3/4), 255-271. https://doi.org/10.1504/IJBM.2023.10053324
3. Chandrakar, R., Raja, R., Miri, R., Sinha, U., Kushwaha, A. K. S., Raja, H. Enhanced the Moving Object Detection and Object Tracking for Traffic Surveillance Using RBF-FDLNN and CBF Algorithm. Expert Systems with Applications, 2022, 191(Apr.), 116306. https://doi.org/10.1016/j.eswa.2021.116306
4. Cherri, A. K., Nazar, A. S. Class-Associative Multiple Target Recognition for Highly Compressed Color Images in a Joint Transform Correlator. Optical Engineering, 2022, 61(12), 123102. https://doi.org/10.1117/1.OE.61.12.123102
5. Jaiswal, P. S., Choudhry, M. S. WMFLICM: A Robust Algorithm for SAR Image Segmentation Using Hybrid Spatial Information. IETE Journal of Research, 2023, 69(6), 3242-3251. https://doi.org/10.1080/03772063.2021.1913072
6. Ketsoi, V., Raza, M., Chen, H., Yang, X. SREFBN: Enhanced Feature Block Network for Single-Image Super-Resolution. IET Image Processing, 2022, 16(12), 3143-3154. https://doi.org/10.1049/ipr2.12546
7. Lahoti, G., Ranjan, C., Chen, J., Yan, H., Zhang, C. Convolutional Neural Network-Assisted Adaptive Sampling for Sparse Feature Detection in Image and Video Data. IEEE Intelligent Systems, 2023, 38(1), 45-57. https://doi.org/10.1109/MIS.2022.3215779
8. Lalapura, V. S., Amudha, J., Satheesh, H. S. Recurrent Neural Networks for Edge Intelligence: A Survey. ACM Computing Surveys, 2022, 54(4), 91.1-91.38. https://doi.org/10.1145/3448974
9. Lee, Y., Shin, H. S., Kim, J. W., Lee, J. A Convolutional Neural Network for Classification of Stimuli Based on Stretchable Mechanical Sensor. IEEE Sensors Journal, 2023, 23(17), 20338-20347. https://doi.org/10.1109/JSEN.2023.3296410
10. Lin, P. Y., Ma, X. S., Peng, X. D. Ship Target Match Method Based on Simulation Template and SuperGlue Feature Matching. Computer Simulation, 2023, 40(11), 11-15. https://doi.org/10.3969/j.issn.1006-9348.2023.11.003
11. Mani, V. R. S., Saravanaselvan, A., Arumugam, N. Performance Comparison of CNN, QNN and BNN Deep Neural Networks for Real-Time Object Detection Using Zynq FPGA Node. Microelectronics Journal, 2022, 119(Jan.), 105319. https://doi.org/10.1016/j.mejo.2021.105319
12. Nie, Q., Malik, S. CNNFlow: Memory-Driven Data Flow Optimization for Convolutional Neural Networks. ACM Transactions on Design Automation of Electronic Systems, 2023, 28(3), 40-75. https://doi.org/10.1145/3577017
13. Radmanesh, M., Ghorbanzadeh, H., Rezaei, A. A., Jalili, M., Yu, X. Learning Asymmetric Embedding for Attributed Networks via Convolutional Neural Network. Expert Systems with Applications, 2023, 219(Jun.), 119659. https://doi.org/10.1016/j.eswa.2023.119659
14. Ranjith, C. P., Hardas, B. M., Mohideen, M. S. K., Raj, N. N., Robert, N. R., Mohan, P. Robust Deep Learning Empowered Real-Time Object Detection for Unmanned Aerial Vehicles Based Surveillance Applications. Journal of Mobile Multimedia, 2023, 19(2), 451-476. https://doi.org/10.13052/jmm1550-4646.1925
15. Salgado, I., Guarneros-Sandoval, A., Ballesteros, M., Rodriguez-Santillan, J., Chairez, I. Lyapunov Stable Learning Laws for Multilayer Recurrent Neural Networks. Neurocomputing, 2022, 491(Jun. 28), 644-657. https://doi.org/10.1016/j.neucom.2021.12.041
16. Schller, F. E. T., Nalpantidis, L., Blanke, M. Buoy Light Pattern Classification for Autonomous Ship Navigation Using Recurrent Neural Networks. IEEE Transactions on Intelligent Transportation Systems, 2022, 23(7), 9455-9465. https://doi.org/10.1109/TITS.2021.3122275
17. Sheikh, A. B., Baru, A., Desai, S. S., Mangale, S. Object Detection Based on Multi-Modal Adaptive Fusion Using YOLOv3. Journal of Applied Remote Sensing, 2022, 16(2), 024523. https://doi.org/10.1117/1.JRS.16.024523
18. Sitaula, C., Xiang, Y., Aryal, S., Lu, X. Scene Image Representation by Foreground, Background and Hybrid Features. Expert Systems with Applications, 2021, 182(11), 115285. https://doi.org/10.1016/j.eswa.2021.115285
19. Wang, L., Shoulin, Y., Alyami, H., Laghari, A. A., Rashid, M., Almotiri, J. A Novel Deep Learning-Based Single

Shot Multibox Detector Model for Object Detection in Optical Remote Sensing Images. Geoscience Data Journal, 2024, 11(3), 237-251. https://doi.org/10.1002/gdj3.162

20. Weerakody, P. B., Wong, K. W., Wang, G. Cyclic Gate Recurrent Neural Networks for Time Series Data with Missing Values. Neural Processing Letters, 2023, 55(2), 1527-1554. https://doi.org/10.1007/s11063-022-10950-2
21. Windisch, A., Simon, P. L. Global Bifurcations in a Dynamical Model of Recurrent Neural Networks. Applications of Mathematics, 2023, 68(1), 35-50. https://doi.org/10.21136/AM.2022.0158-21
22. Yin, H., Li, Y., Sun, M., Ibrar, L., Teng, L. Data Visualization Analysis Based on Explainable Artificial Intelligence: A Survey. IJLAI Transactions on Science and Engineering, 2024, 2(2), 13-20. https://doi.org/10.1007/978-3-662-68313-2_2
23. Yin, L., Wang, M., Shafiq, L., Teng, A. A., Laghari, M. F., Khan, M. F. G2Grad-CAMRL: An Object Detection and Interpretation Model Based on Gradient-Weighted Class Activation Mapping and Reinforcement Learning in Remote Sensing Images. IEEE Journal of Selected Topics in Applied Earth Observations and Remote Sensing, 2023, 16, 3583-3598. https://doi.org/10.1109/JSTARS.2023.3241405
24. Zheng, Q., Zhao, P., Zhang, D., Wang, H. MR-DCAE: Manifold Regularization-Based Deep Convolutional Autoencoder for Unauthorized Broadcasting Identification. International Journal of Intelligent Systems, 2021, 36(12), 7204-7238. https://doi.org/10.1002/int.22586
25. Zheng, Q. H., Tian, X., Yang, M., Wu, Y., Su, H. PAC-Bayesian Framework Based Drop-Path Method for 2D Discriminative Convolutional Network Pruning. Multidimensional Systems and Signal Processing, 2020, 31(3), 793-827. https://doi.org/10.1007/s11045-019-00686-z